Arabian Journal of Geosciences (2020) 13:573
https://doi.org/10.1007/s12517-020-05619-w

ORIGINAL PAPER

# Assessment of gold mineralisation in Osu–Amuta–Itagunmodi areas, Southwestern Nigeria

Jerry O. Olajide-Kayode [1,2] · Shakirat O. Mustapha [1,3] · Akinade S. Olatunji [2] · Olugbenga A. Okunlola [2]

Received: 2 January 2020 / Accepted: 22 June 2020
© Saudi Society for Geosciences 2020

## Abstract

Gold is artisanally mined from eluvial deposits within Osu–Amuta–Itagunmodi areas of Ilesa Schist Belt, southwestern Nigeria. Mine site selection and mining operations are done without any understanding of mode of occurrence, compositional characteristics and extent of gold mineralisation. The present study was aimed at determining the host lithologies, extent and associated geochemical features of the gold mineralisation. Fifty rock samples were cut into thin section for examination and analysed using inductively coupled plasma–mass spectrometry (ICP-MS). Forty-eight soil samples collected from Artisanal Gold Mine (AGM) pits to a depth of 5 m ($n$ = 9), and along defined horizontal profile lines from the mine pits ($n$ = 39) were analysed for elemental constituents, and mineralogical compositions in vertical profile samples using ICPMS and X-ray diffraction (XRD) techniques, respectively. The quartz-biotite schist, quartzite, talc-chlorite schist and amphibolite had Au concentration (ppb) that ranged from 1.3 to 14.4 (average 3.95), BDL–0.9 (average 0.63), 0.9–4.6 (average 2.18) and 0.5–2.7 (average 1.56), respectively. Vertical and lateral profile soil samples were Osu: 4.5–7.6 (average 6.17) and 0.9–78.8 (average 8.54); Amuta: 4.1–6.8 (average 5.2) and 2.8–19.8 (average 7.40); and Itagunmodi 3.9–13.2 (average 7.43) and 0.5–14.8 (average 4.33). Evaluation of the horizontal profile soils revealed higher Au concentrations than the artisanal mine workings, indicating additional mineralisation potentials in the study area. Au concentrations were in the order of quartz-biotite schist > talc-chlorite schist > amphibolite >> quartzite, with anomalous concentrations detected in quartz-biotite and talc-chlorite schists. Elevated concentrations also occurred in residual soils overlying quartzite and amphibolite lithologies. Mineralisation is hydrothermal in nature, extends beyond current artisanal mine workings and has potential for further exploration.

**Keywords** artisanal mining · Ilesa Schist Belt · hydrothermal alteration · gold mineralization potential

## Introduction

The Proterozoic Schist Belts of Nigeria, with north–south trending features confined to the western half, are known to host economic minerals including gold (Obaje 2009). Gold mineralisation in these belts (Maru, Anka, Malele, Tsohon Birnin Gwari-Kwaga, Gurmana, Bin Yauri, Okolom Dogondaji and Iperindo; Fig. 1) has been described as hydrothermal type (Oyinloye 1995, 1997; Oyinloye and Steed 1996; Akande et al. 1988). Studies have been conducted on the geochemical characteristics of primary (lode) gold mineralisation near Tsohon Birnin Gwari (Garba, 2002), Orle district within the Igarra schist belt (Adepoju and Adekoya 2011), gold-bearing quartz veins in Maru schist belt (Oke et al. 2014) and Iperindo in Ilesa area (Oyinloye 1997, 2002; Oyinloye and Steed 1996). Akinlalu et al. (2018) also conducted an aeromagnetic mapping of basement structures for mineralisation characterisation in the Ilesa Schist Belt. Although gold production in Nigeria began in 1913 and peaked in the 1930s (Ministry of Mines and Steel Development (MMSD) 2004), gold mining operations are predominantly artisanal with the aid of crude tools and processes (Fig. 2). These activities, common in areas with placer

Responsible Editor: Domenico M. Doronzo

**Electronic supplementary material** The online version of this article (https://doi.org/10.1007/s12517-020-05619-w) contains supplementary material, which is available to authorized users.

✉ Jerry O. Olajide-Kayode
jolugbn@gmail.com

[1] Department of Geosciences, Pan African University Life and Earth Sciences Institute (PAULESI), University of Ibadan, Ibadan, Nigeria

[2] Department of Geology, University of Ibadan, Ibadan, Nigeria

[3] Department of Geology, Kwara State University, Malete, Nigeria

Published online: 01 July 2020

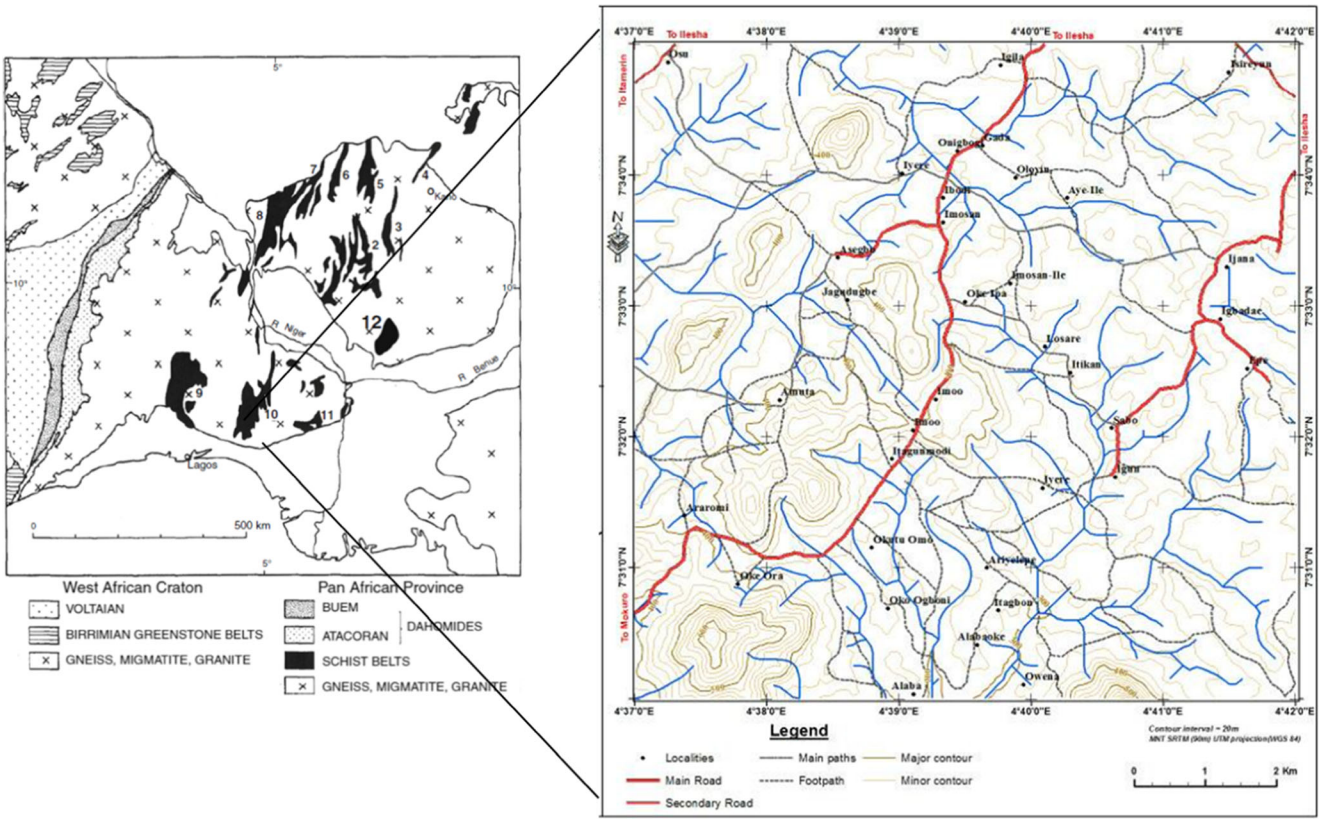



**Fig. 1** The study area within the framework of the regional geology of West Africa (modified after Wright 1985). 1—Zungeru-Birnin Gwari, 2—Kusheriki-Kushaka, 3—Karaukarau, 4—Kazaure, 5—Wonaka, 6—Maru, 7—Anka, 8—Zuru, 9—Iseyin-Oyan River, **10—Ilesa**, 11—Igarra, 12—Muro Hills

gold mineralisation, are carried out without any scientific knowledge of the mode of occurrence and style of mineralisation of the gold deposit.

In the Ilesa Schist Belt, sites of placer gold have been reported in many areas west of the Ifewara–Zungeru Fault System (Fig. 3), a 550-km-long NNE–SSW fault which runs along the length of the belt and terminates at the edge of River Niger (Oyinloye and Steed 1996). These include minor occurrences of residual gold in soils at amphibolite–pegmatite contact in Ajegunle-Awa, and in panned soil and stream sediment concentrates in Bishewa, Koro and Wara areas (MMSD 2004); elevated concentration of gold in stream sediments of Itagunmodi (Akintola et al. 2013). These placers are actively worked through artisanal gold mining, with no scientific approach to mine site selection or adequate geologic information about the gold occurrences. The present study is aimed at establishing the lithological relationship, mode of occurrence and geochemical signature of gold mineralisation around Osu, Itagunmodi and Igun areas within the Ilesa Schist Belt, Southwestern Nigeria. An assessment was also undertaken in order to identify possible additional mineralization potentials in the area.

## Study area description

The study area, bounded by latitudes 04°37′00″–04°42′00″ and longitudes 07°30′00″–07°35′00″, lies about 35 km west of Ilesa town. It is underlain by the rocks typical of the Basement Complex of southwest Nigeria and characterized by the tropical rain forest climate.

The artisanal miners haphazardly select Artisanal Gold Mine (AGM) pit sites, where gold-bearing saprolitic layers are panned (Fig. 2b) to extract gold and associated heavy minerals. Locally fabricated sluice boxes are also employed in the beneficiation of the saprolite slurries where carpets, which act as traps, are placed in these boxes while the slurries are run over them (Fig. 2a).

## Methodology

A geological mapping of the study area was undertaken on a scale of 1:10,000. Fifty rock samples (quartz-biotite schist, 12; talc-chlorite schist, 6; quartzite, 10; and amphibolite, 22) were analysed for whole rock composition, while 48 soil samples were collected for analysis. The soils were obtained from selected artisanal mining pits (down the excavated pit profile) at




**Fig. 2** (**a**) Typical artisanal mining process in the study area using a sluice box. (**b**) Gold (arrowed) panned from saprolite, with associated heavy minerals (black) (pen cover used as scale)

various depths. Three samples each were collected from Orogo and Itagunmodi pits at depths of 0 m (top), 1 m and 2 m, while at the Amuta pit, samples were collected at the top, 1.5 m and 3.5 m depths, respectively. In addition, soil samples were obtained at a 0–30 cm depth along a profile defined at 100-m intervals in the North, East, South and West directions at the pits in Orogo ($n$ = 19), and 50 m to the West and East directions at Amuta ($n$ = 10) and Itagunmodi ($n$ = 10) (Fig. 4, Table 3, Online Resource I–III).

The soil samples were air-dried at room temperature, disaggregated and sieved to extract the <75-μm fractions. The concentration of Au and associated elements were analysed by inductively coupled plasma–mass spectrometry after lithium metaborate fusion digestion at Bureau Veritas Minerals Laboratory, Vancouver, Canada. The mineralogy of the samples obtained from the vertical profiles was determined by X-ray diffraction method at the University of Poitier XRD Laboratory, France. The pulverised rock samples were also analysed using inductively coupled plasma–mass spectrometry after lithium metaborate fusion digestion at the Bureau Veritas Minerals Laboratory. Operating conditions for the XRD and ICP analyses are according to Bish (1994) and Zhu et al. (2009), respectively. The results of the geochemical analysis were interpreted using statistical analysis.

## Results and discussions

### Geological setting

The study area is underlain by amphibolite, talc schist and metasedimentary units of quartzite and quartz-biotite schist (Fig. 5). The quartz-biotite schist (Fig. 6) is the dominant lithology but poorly exposed, occurring as weathered, often low-lying outcrops in the northwestern and most of the eastern parts of the study area. Quartz, biotite and plagioclase are the main minerals visible in hand specimen while in thin section, quartz occur as subhedral to euhedral hetero-granular grains, with elongate biotite grains defining the foliation in the schists. Quartzites occur as northerly trending ridges in the western and southeastern parts, composed mainly of medium to coarse interlocking quartz grains (Fig. 7) and are weathered and highly jointed. The talc schists, which were of the talc-chlorite variety (Fig. 8), occurred as discontinuous enclaves within amphibolites and the quartz-biotite schist, with characteristic fine-grained texture and soapy feel. Optical examination of the rocks revealed a predominantly talc composition, which occurs mostly as a colourless mosaic in plane polarized light and pale shades of pink and green under crossed polars. Chlorite, indicative of low-grade metamorphism, occurs as the secondary mineral in the samples. Amphibolites in the study area are of the massive textural variety, occurring mostly as discontinuous lensoid bodies of small to large boulders, composed of hornblende, with subordinate plagioclase and epidote (Fig. 9). Accessory titanite was observed in some of rocks.

### Description of the gold mine pits

The gold mine pit at Orogo was located within the quartzite/quartz-biotite schist terrain; the topsoil obtained at 0–20 cm depth was brown, fine-medium grained sand containing decomposed organic matter. Dark-brown, medium-grained sand occurred at 1 m while gold-bearing saprolite was encountered at 2 m depth (Fig. 10). At the Amuta pit, reddish brown to darkened brown sandy-clay was observed, and gold-bearing saprolite was encountered at 3.5 m (Fig. 11). The mine pit at Itagunmodi is composed of organic matter–bearing topsoil at 0–30 cm, with dark reddish-brown, medium-grained clayey-sand occurring till 2 m depth, where gold-bearing

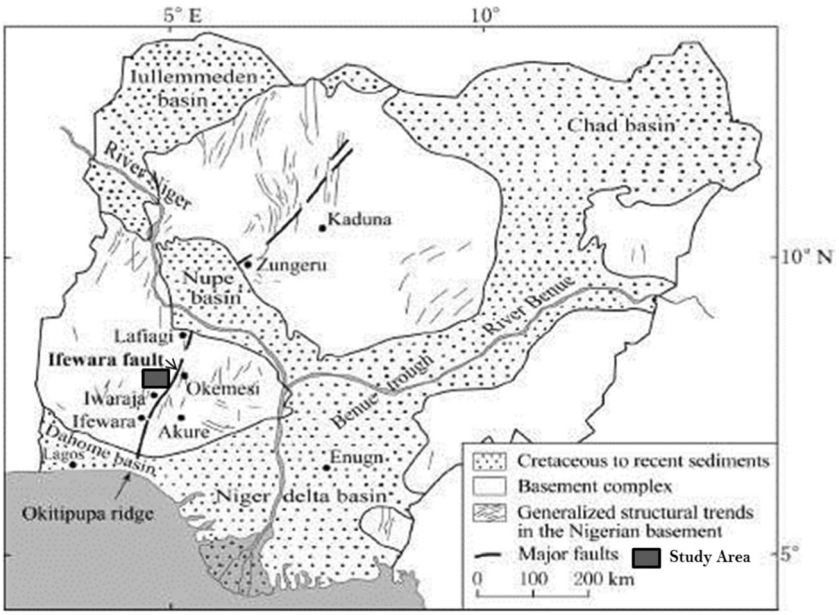



**Fig. 3** The Ifewara–Zungeru Fault in the western half of Nigeria (Akpan and Yakubu 2010)

saprolite occurred (Fig. 12). The pits at Amuta and Itagunmodi were underlain by amphibolite lithology (Fig. 13).

## Mineralogy of soil samples

Quartz (34.15–84.91%) with subordinate kaolinite (10.42–38.39%) and hematite (2.40–27.46%) were the major minerals identified by XRD analysis in the nine (9) vertical profile samples from the AGM pits. Minor amounts of mica (1.00–5.81%) were also detected in most of the samples (Table 1). Kaolinite forms as a result of weathering or hydrothermal alteration of aluminium-rich silicates. Hence, rocks that contain feldspars will usually weather to give kaolinite (Deer et al. 1992). The kaolinite is believed to be a by-product of weathering/hydrothermal alteration of feldspars of the quartz-biotite schist and amphibolites in the study area. The hematite resulted from lateritisation process and alteration of Fe-bearing minerals in the amphibolite.

## Trace elemental composition

A summary of the concentration of gold and other associated elements in rocks and soils of the studied area are presented in Tables 2 and 3. The concentration (ppb) of Au in the amphibolites, quartzites, talc-chlorite schists and quartz-biotite schists ranged from 0.5 to 2.7, 0.5–0.9, 0.9–4.6 and 1.3–14.4, with mean values 1.56 ± 0.63, 0.63 ± 0.23, 2.18 ± 1.70 and 3.95 ± 4.20, respectively. The concentration of Hg was below detection limit (BDL) and that of Ag preponderantly below detection limit (Table 2). In the soils obtained at and around the AGM pits, Au concentration (ppb) in vertical profile samples from Orogo, Amuta and Itagunmodi ranged from 4.5 to 7.6, 4.1–6.8 and 3.9–13.2, respectively, with average values of 6.17, 6.78 and 7.43. Soil samples from the horizontal profile have Au concentrations in the range of 0.9–78.8, 2.8–19.8 and 0.5–14.8, respectively. The concentrations of other elements in the rocks and soils are presented in Online Resource IV and V–VII.

## Spatial distribution and variation of Au

Results from whole rock geochemical analysis revealed that the concentration of Au in rocks of the study area were in the order quartz-biotite schist > talc-chlorite schist > amphibolite >> quartzite. The fissile nature of the schists could have facilitated easier passage of Au-bearing hydrothermal fluid and subsequent deposition of higher concentration of Au relative to the amphibolites and quartzites. This is believed to be responsible for the higher concentration of Au detected in the schistose rocks relative to the other rock units (Fig. 14). When compared with the concentration of Au in the average crust, majority of the rocks displayed low abundances of Au, with very few of the schistose rocks displaying concentrations exceeding the crustal threshold (Table 2). These anomalous gold concentration zones are depicted in Fig. 14.

In the Orogo area, the three samples collected down-pit at the mine recorded concentrations above the crustal average, and the concentration was observed to increase with depth (Online Resource V, Fig. 15). Soils from six (6) sampling sites on the horizontal profile (S4, S13, S14, S15, S17 and S22) had Au concentrations that exceeded the crustal average (Fig. 16). At Amuta AGM, the Au concentration in samples obtained from the vertical profile increased slightly with depth and exceeded the crustal average. All but one (S30) of the

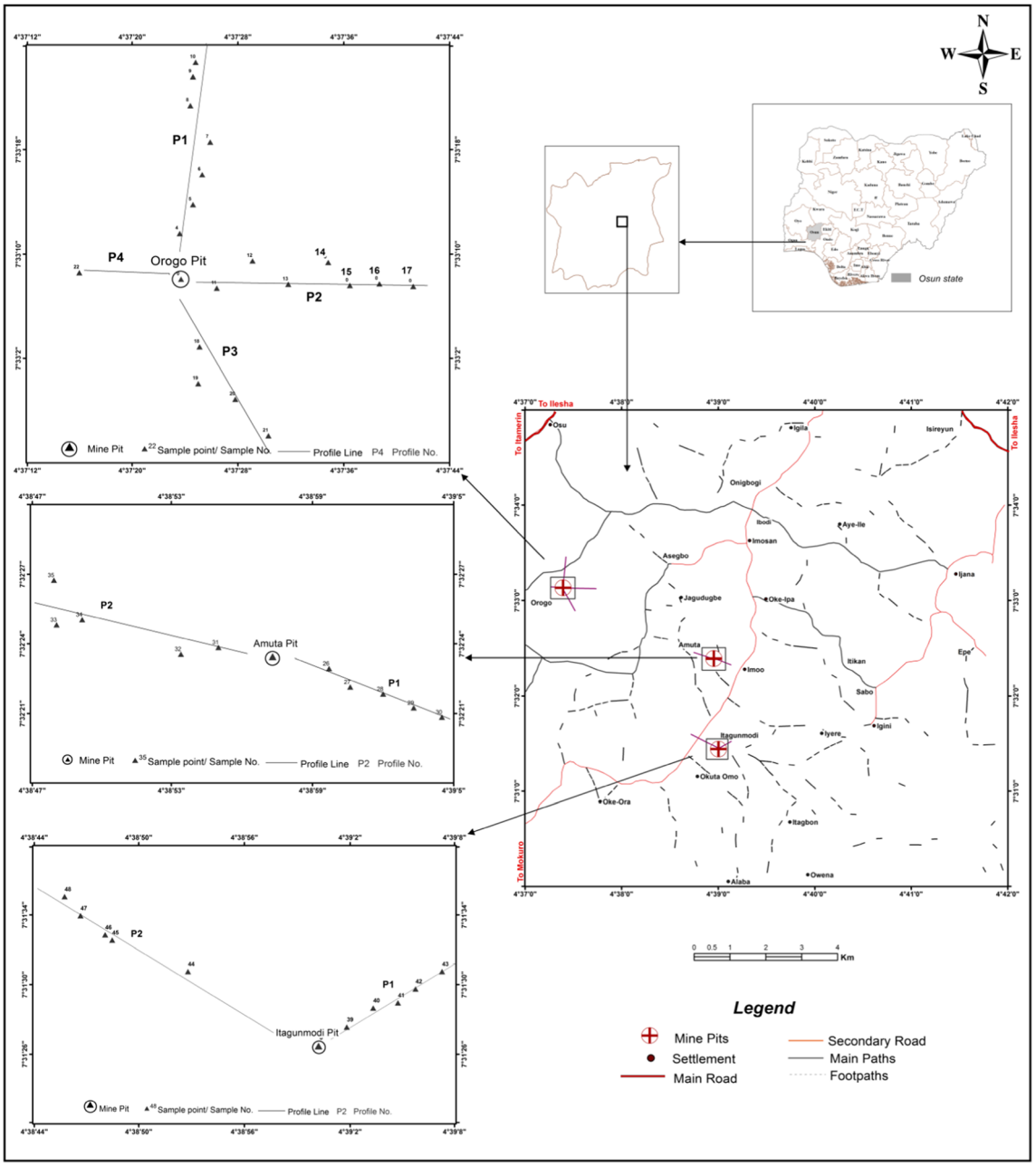



**Fig. 4** Horizontal profile sampling points at Orogo (Osu), Amuta and Itagunmodi AGM pits

sampling points on the lateral profile had Au concentrations higher than the average crust (Online Resource VI, Figs. 15 and 17). At 1-m depth, there was a marked increase in the concentration of Au (13.2 ppb) compared with the top of the AGM pit (5.2 ppb) at Itagunmodi, followed by a sharp decrease in concentration at 2 m depth (3.9 ppb) (Fig. 15). Three sampling locations (S40, S47 and S48) on the horizontal profile recorded concentrations above the crustal average (Online Resource VII, Fig. 17).

The concentration of Au in samples obtained from the lateral profiles was also compared with the Au concentration in the saprolitic layers from which the Au was panned at each active AGM (Online Resource V, VI and VII). At Orogo, the Saprolitic Profile Value (SPV) of Au was 7.6 ppb, while those of Amuta and Itagunmodi were 6.8 and 3.9 ppb, respectively. When compared, four (4) of the samples obtained from the horizontal profile at Orogo (S4, S13, S14 and S15) exceeded the SPV (Table 3; Fig. 16). Three (3) of the samples from Amuta (S29, S31 and S34) and Itagunmodi (S40, S47 and S48) horizontal profiles exceeded their respective SPVs (Table 3; Figs. 17 and 18).




**Fig. 5** Field occurrences of (**a**) quartz-biotite schist, (**b**) quartzite, (**c**) talc-chlorite schist and (**d**) amphibolite

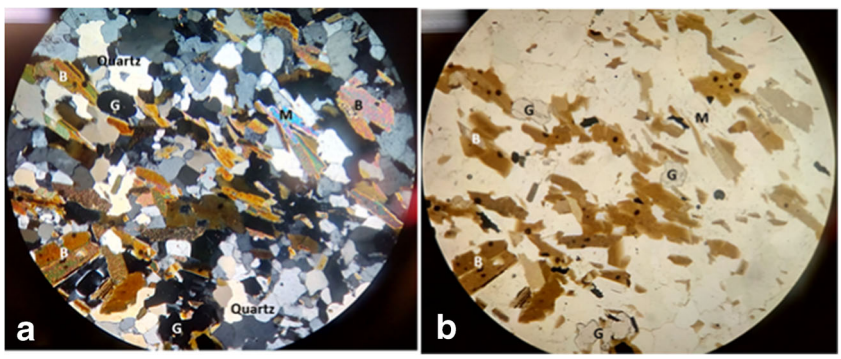



**Fig. 6** Photomicrographs of quartz-biotite schist (**a**) under crossed-polar and (**b**) plane-polarised light (B, biotite; Q, quartz; G, garnet; M, muscovite; magnification ×40)

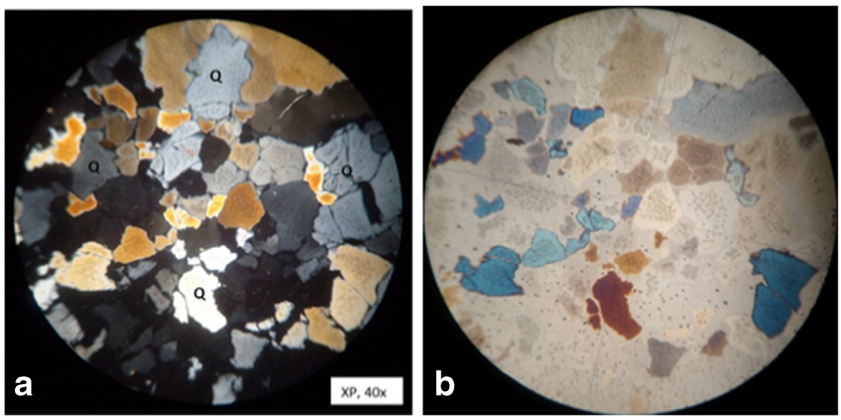



**Fig. 7** (**a**) Crossed nicol and (**b**) plane-polarised photomicrographs of quartzite (magnification ×40)

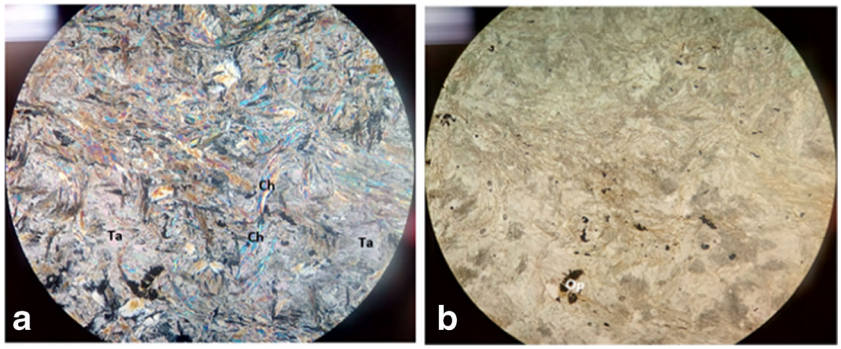



**Fig. 8** (**a**) Crossed nicol and (**b**) plane-polarised photomicrographs of talc-chlorite schist showing inclusions of chlorite and minor opaques in a mosaic of talc (Ta—talc, Ch—chlorite, Op—opaque; magnification ×100)

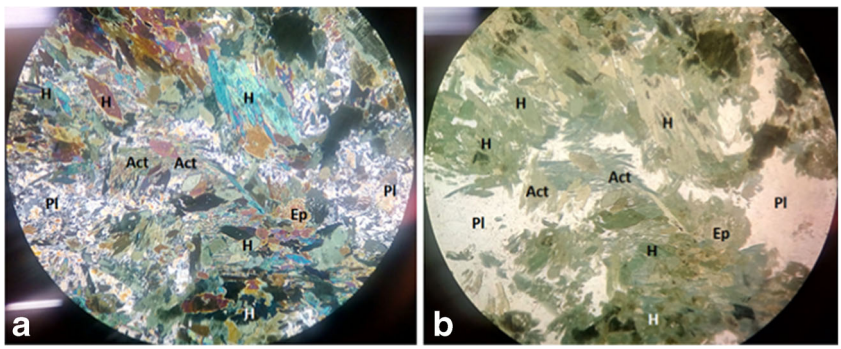



**Fig. 9** Amphibolite under crossed-polar (**a**) and plane-polarised light (**b**) (H—hornblende, Act—actinolite, Ep—epidote, Pl—plagioclase; magnification ×40)

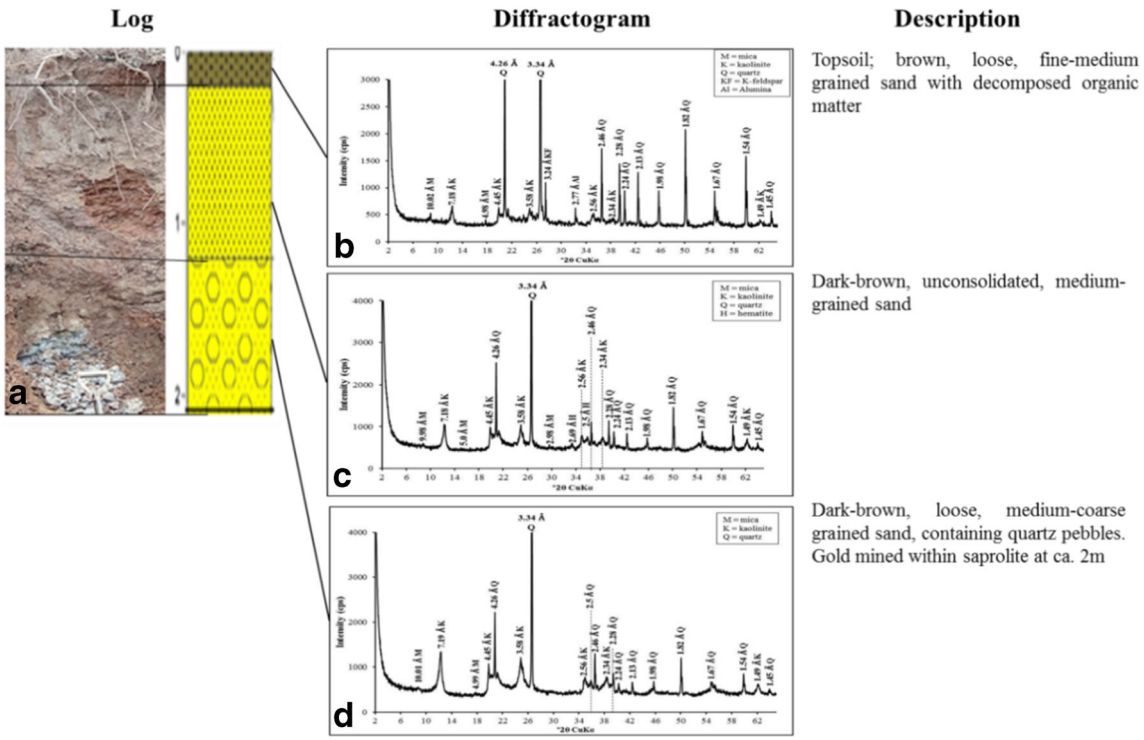



**Fig. 10** Pit profile mineralogical composition of Orogo AGM pit

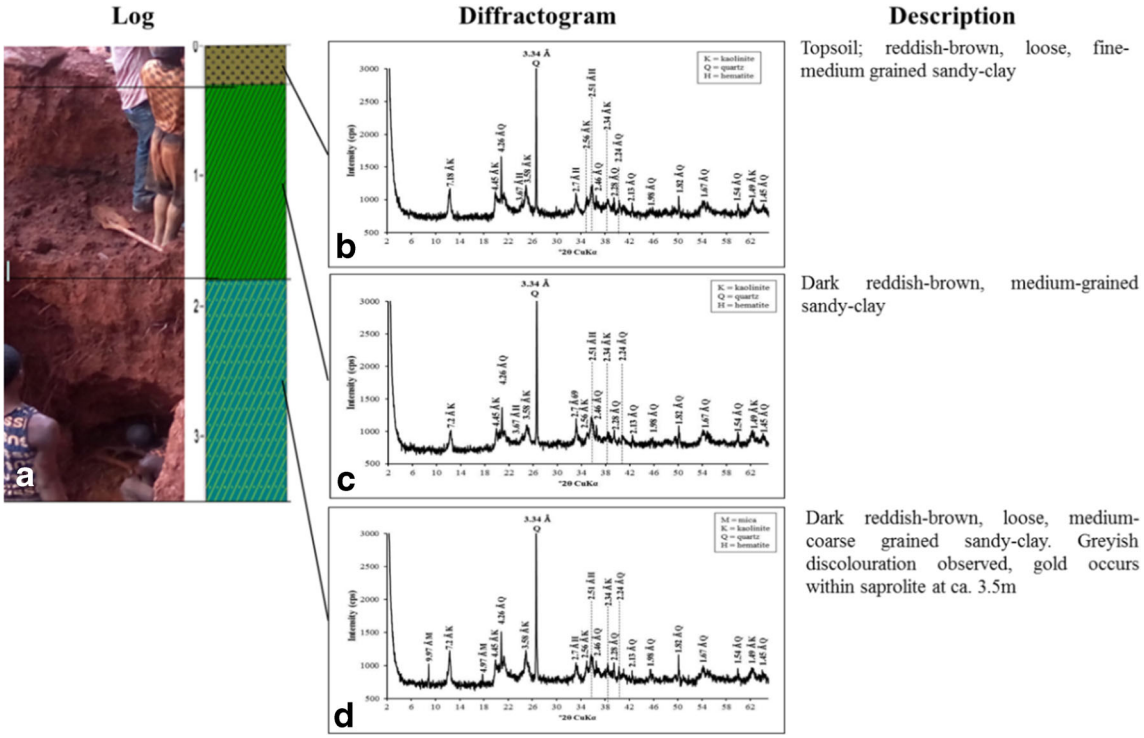



**Fig. 11** Pit profile mineralogical composition of Amuta AGM pit

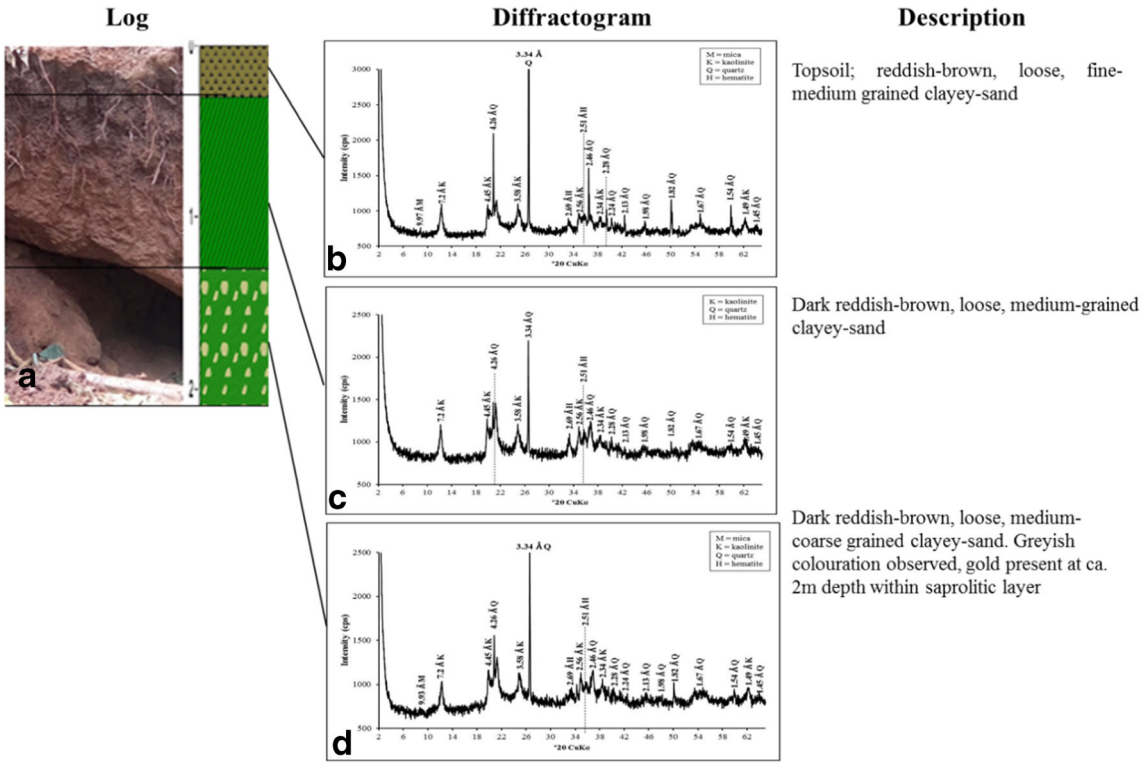



**Fig. 12** Pit profile mineralogical composition of Itagunmodi AGM pit

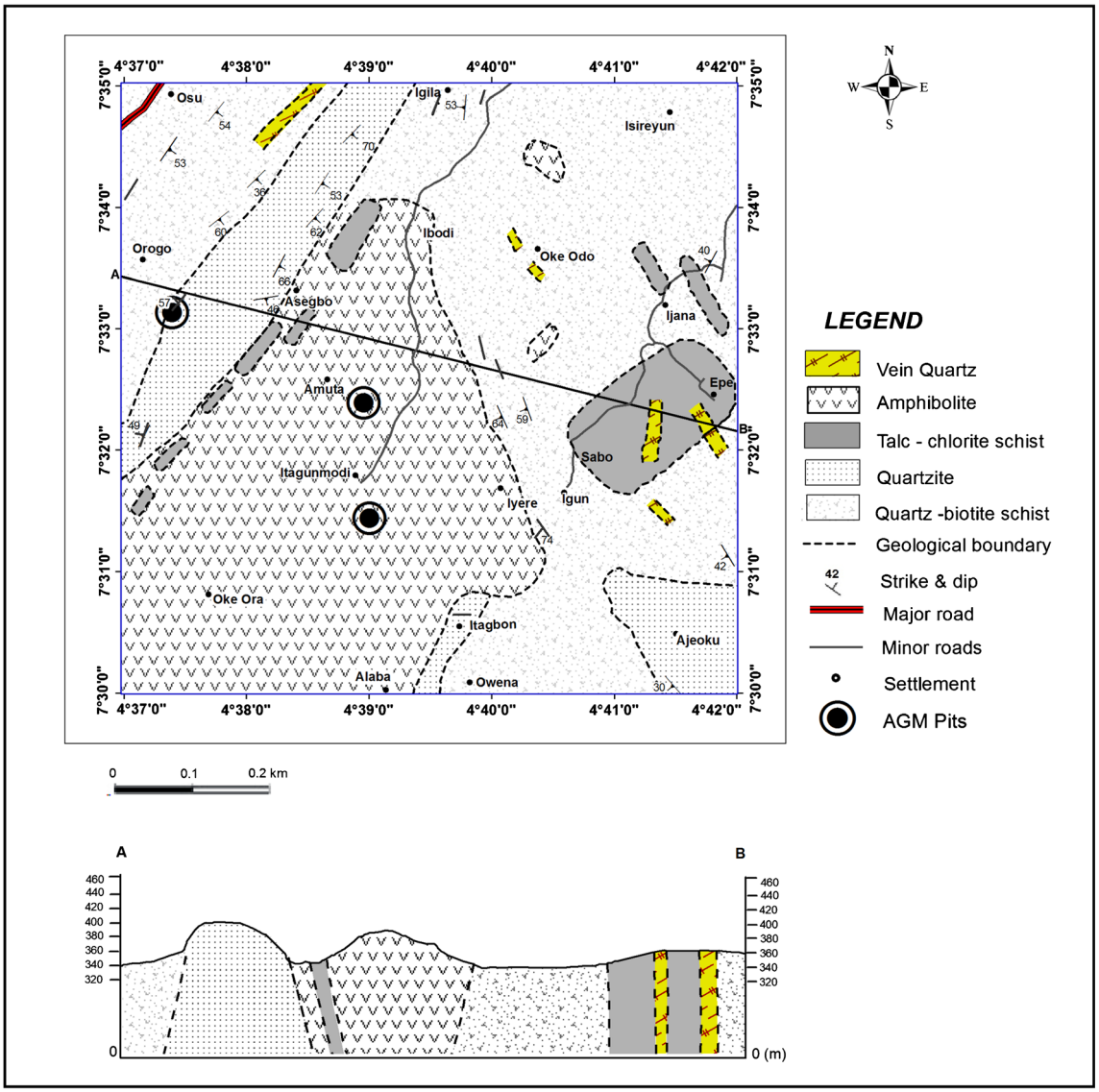



**Fig. 13** Geologic map of the study area showing AGM pits

**Table 1** Mineralogical composition of soil samples from vertical profiles in the AGM pits

| Sample | Depth (m) | Location | Lithology | M | K | Q | H |
|---|---|---|---|---|---|---|---|
| S1* | Top | Orogo Pit | Quartzite/quartz-biotite schist | 2.86 | 10.42 | 77.88 | – |
| S2 | 1 | | | 1 | 11.69 | 84.91 | 2.4 |
| S3 | 2 | | | 2.86 | 15.06 | 82.08 | – |
| S4 | Top | Amuta Pit 1 | Amphibolite | – | 32.19 | 58.42 | 9.39 |
| S5 | 1.5 | | | – | 16.5 | 67.51 | 15.98 |
| S6 | 3.5 | | | 5.81 | 25.83 | 60.14 | 8.23 |
| S7 | Top | Itagunmodi Pit | | 1.74 | 20.98 | 68.72 | 8.56 |
| S8 | 1 | | | – | 38.39 | 34.15 | 27.46 |
| S9 | 2 | | | 1.83 | 24.81 | 59.37 | 13.99 |

*M* mica, *K* kaolinite, *Q* quartz, *H* hematite

*Minor amounts of k-feldspar and alumina detected

**Table 2** Summary of trace element composition in rocks of Osu and environs

| Elements (ppm) | Amphibolite ($n$ = 22) | | Quartzites ($n$ = 10) | | Talc-chlorite schist ($n$ = 6) | | Quartz-biotite schist ($n$ = 12) | | |
|---|---|---|---|---|---|---|---|---|---|
| | Range | Mean ± SD | Range | Mean ± SD | Range | Mean ± SD | Range | Mean ± SD | ACV |
| Au (ppb) | 0.5–2.7 | 1.56 ± 0.63 | 0.5–0.9 ($n$ = 3) | 0.63 ± 0.23 | 0.9–4.6 ($n$ = 4) | 2.18 ± 1.70 | 1.3–14.4 | 3.95 ± 4.20 | 4 |
| Hg | BDL | – | BDL | – | BDL | – | BDL | – | 0.08 |
| Ag | BDL-0.2 | 0.15 ± 0.05 | BDL | – | BDL | – | BDL | – | 0.07 |
| Cu | 22.3–41.1 | 34.35 ± 5.35 | 11.20–12.30 | 12.17 ± 1.22 | 3.0–35.0 | 26.0 ± 24.16 | 21.0–46.20 | 26.23 ± 8.22 | 55 |
| Sb | 0.1–0.4 | 0.19 ± 0.10 | 0.4–0.5 | 0.44 ± 0.05 | BDL | – | 0.1–0.3 | 0.13 ± 0.06 | 0.2 |
| As | 0.5–3.2 | 1.48 ± 0.80 | 1.0–1.7 | 1.29 ± 0.20 | BDL | – | 0.6–3.2 | 2.47 ± 0.98 | 1.8 |
| Mo | 0.4–4.5 | 2.17 ± 1.22 | 0.7–0.9 | 0.8 ± 0.05 | BDL | – | 0.3–1.7 | 0.74 ± 0.54 | 1.5 |
| Pb | 3.4–25.2 | 15.55 ± 6.66 | 0.6–0.8 | 0.65 ± 0.08 | 0.2–2.0 | 0.72 ± 0.65 | 3.0–18.6 | 6.63 ± 6.18 | 12.5 |
| Zn | 20.0–52.0 | 39.36 ± 9.94 | 2.0–4.0 | 2.30 ± 0.67 | 6.0–34.0 | 16.17 ± 9.99 | 40.0–52.0 | 46.253.22 | 70 |
| Ni | 29.0–102.0 | 80.55 ± 24.60 | BDL | – | 833.0–1568.0 | 1246.0 ± 283.4 | BDL–100.0 | 48.0 ± 32.64 | 75 |
| Co | 14.2–43.2 | 35.03 ± 9.53 | 1.2–1.5 | 1.36 ± 0.10 | 65.0–87.9 | 75.87 ± 10.04 | 13.3–43.4 | 20.81 ± 12.60 | 25 |
| Cd | BDL | – | BDL | – | BDL | – | BDL | – | 0.2 |

*ACV* average crustal value (Turekian and Wedepohl 1961)

**Table 3** Trace element composition in soils from the AGM pits

| Trace elements | Orogo (SPV—7.6 ppb) | | | | Amuta (SPV—6.8 ppb) | | | | Itagunmodi (SPV—3.9 ppb) | | | | ACV |
|---|---|---|---|---|---|---|---|---|---|---|---|---|---|
| | Horizontal (n = 19 ) | | Vertical (n = 3) | | Horizontal (n = 10) | | Vertical (n = 3) | | Horizontal (n = 10) | | Vertical (n = 3) | | |
| | Range | Mean ± SD | Range | Mean ± SD | Range | Mean ± SD | Range | Mean ± SD | Range | Mean ± SD | Range | Mean ± SD | |
| Au (ppb) | 0.9–78.8 | 8.54 ± 17.35 | 4.5–7.6 | 6.17 ± 1.28 | 2.8–19.8 | 7.40 ± 4.91 | 4.1–6.80 | 5.2 ± 1.40 | 0.5–14.8 | 4.33 ± 4.51 | 3.9–13.2 | 7.43 ± 4.11 | 4 |
| Hg (ppb) | 45–149 | 97.16 ± 29.12 | 43–85 | 66.00 ± 17.38 | 36.00–146.00 | 95.40 ± 28.71 | 55–71 | 63.7 ± 8.08 | 65–111 | 88.00 ± 12.23 | 29–56 | 38.00 ± 12.73 | 80 |
| Ag (ppb) | 6.0–36 | 25.11 ± 8.25 | 18–34 | 26.33 ± 6.55 | 23.00–123.00 | 64.80 ± 24.66 | 38–85 | 62.3 ± 23.54 | 28–49 | 40.30 ± 5.31 | 16–32 | 24.33 ± 6.55 | 70 |
| Cu (ppm) | 25.35–279.19 | 66.31 ± 56.45 | 20.21–27.31 | 23.52 ± 2.92 | 42.05–108.00 | 77.73 ± 20.39 | 88.11–103.54 | 93.8 ± 8.48 | 45.91–225.46 | 100.75 ± 52.50 | 74.12–83.27 | 79.58 ± 3.94 | 55 |
| Sb (ppm) | 0.03–0.08 | 0.05 ± 0.01 | 0.03 | 0.03 ± 0.00 | 0.17–0.37 | 0.24 ± 0.06 | 0.26–0.38 | 0.3 ± 0.07 | 0.08–0.19 | 0.12 ± 0.04 | 0.08–0.18 | 0.12 ± 0.04 | 0.2 |
| As (ppm) | 0.5–39.8 | 4.70 ± 8.93 | 0.5–1.4 | 0.95 ± 0.45 | 1.10–2.70 | 2.05 ± 0.54 | 1.90–2.70 | 2.3 ± 0.40 | 0.5–2 | 1.01 ± 0.44 | 1–2.8 | 1.73 ± 0.77 | 1.8 |
| Mo (ppm) | 0.43–1.77 | 0.86 ± 0.36 | 0.3–0.8 | 0.48 ± 0.22 | 0.63–1.25 | 0.87 ± 0.19 | 0.88–1.12 | 1.0 ± 0.13 | 0.34–0.96 | 0.55 ± 0.19 | 0.54–0.93 | 0.74 ± 0.16 | 1.5 |
| Pb (ppm) | 14.78–29 | 20.00 ± 3.32 | 12.82–16.67 | 15.36 ± 1.80 | 13.61–21.25 | 18.21 ± 2.11 | 13.25–15.00 | 14.1 ± 0.88 | 16.17–21.87 | 18.13 ± 1.68 | 12.81–15.79 | 14.55 ± 1.27 | 12.5 |
| Zn (ppm) | 22.1–85 | 45.98 ± 14.07 | 26.7–39.4 | 33.00 ± 5.19 | 54.10–81.00 | 71.95 ± 8.75 | 60.7–85.9 | 74.8 ± 12.85 | 63.9–106.3 | 88.56 ± 11.46 | 83–95.2 | 90.33 ± 5.28 | 70 |
| Ni (ppm) | 12.4–49.9 | 24.14 ± 10.69 | 11.9–21 | 17.87 ± 4.22 | 32.30–43.50 | 38.16 ± 3.78 | 39.1–56.4 | 49.0 ± 8.93 | 31.6–71.7 | 48.62 ± 11.38 | 56.2–66 | 60.03 ± 4.28 | 75 |
| Co (ppm) | 5.8–92.7 | 35.59 ± 20.72 | 13.4–19.7 | 16.43 ± 2.58 | 30.10–92.6 | 67.68 ± 18.82 | 44.0–88.2 | 72.2 ± 24.47 | 51.5–86 | 68.68 ± 11.01 | 44.1–74.8 | 56.50 ± 13.21 | 25 |
| Cd (ppm) | 0.01–0.23 | 0.13 ± 0.05 | 0.01–0.08 | 0.04 | 0.02–0.21 | 0.15 ± 0.05 | 0.04–0.12 | 0.1 ± 0.04 | 0.08–0.22 | 0.15 ± 0.04 | 0.03–0.1 | 0.05 ± 0.03 | 0.2 |

*SPV* saprolitic profile value of Au

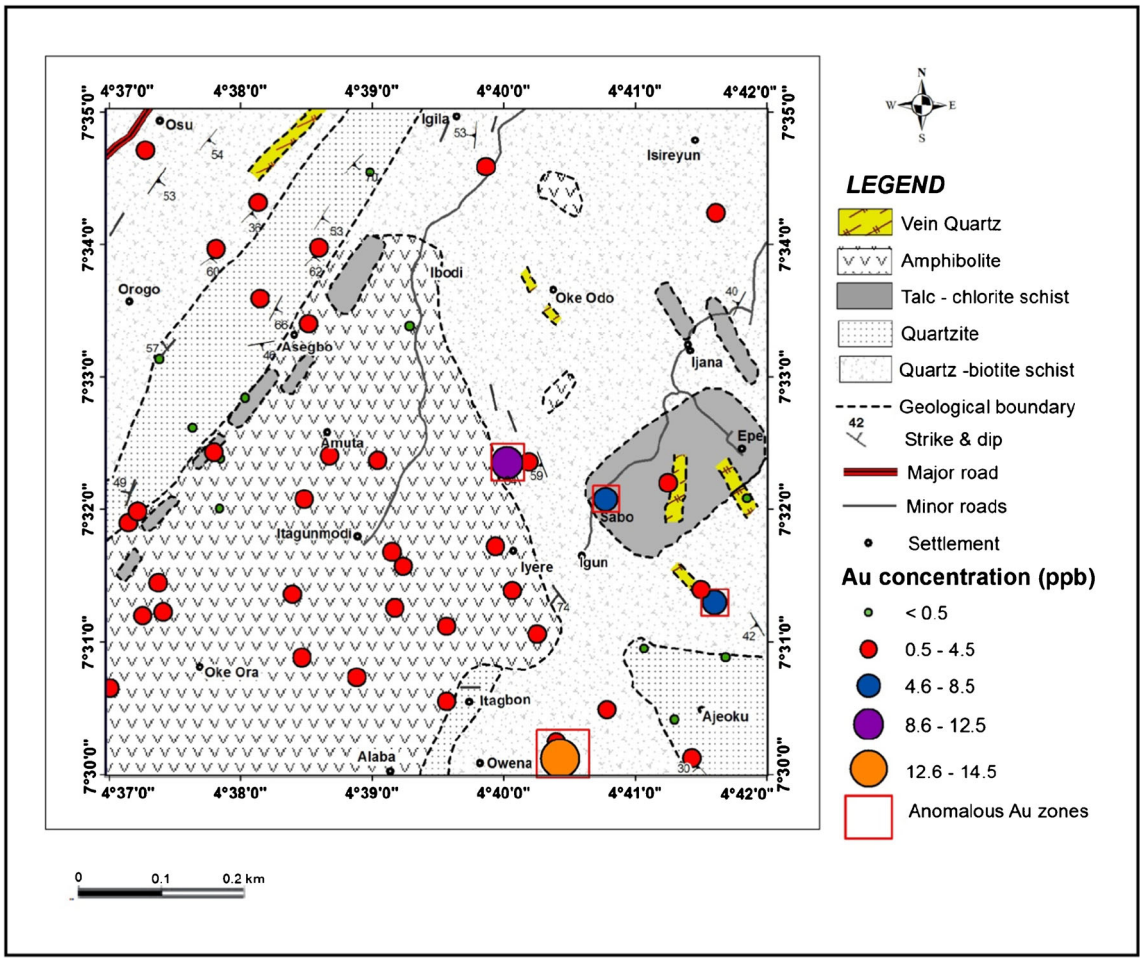



**Fig. 14** Gold concentration and distribution in rocks within Osu–Itagunmodi–Igun area, with anomalous Au zones depicted

## Inter-element relationship between Au and associated elements

In the rocks with anomalous Au concentration, and vertical and lateral profile soils, the relationship between Au and other elements were evaluated using Pearson's correlation matrix and principal component analysis.

Strong positive correlation was established for Au and Zn ($r = 0.704$; $p \leq 0.05$) in quartz-biotite schist. Elemental groupings from principal component analysis (PCA) placed Zn and

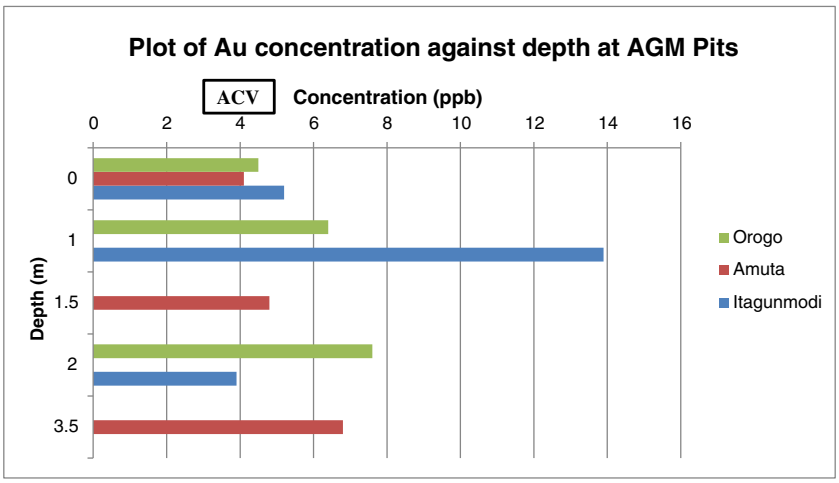



**Fig. 15** Depth–concentration variation of Au in vertical profile samples from the AGM pits

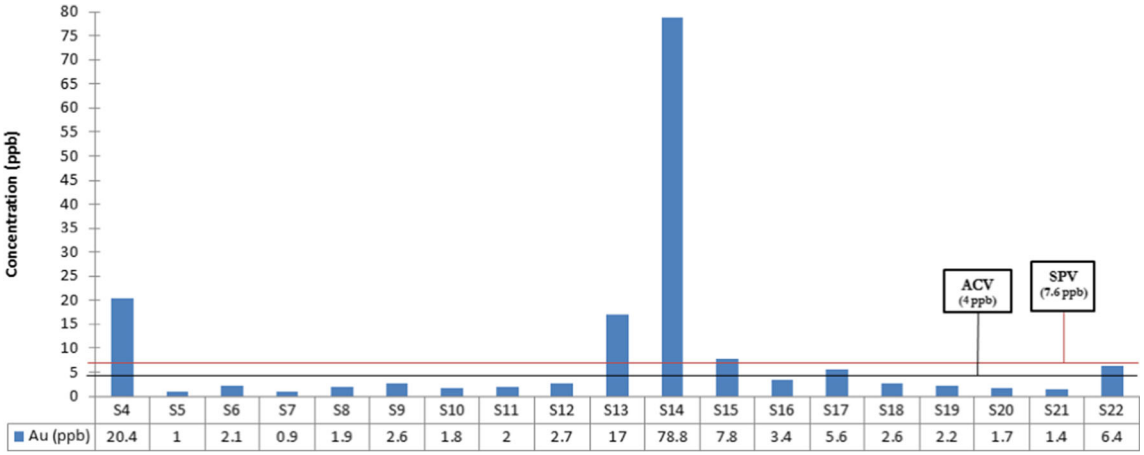



**Fig. 16** Comparison of Au concentration in Orogo lateral profile sample with ACV and SPV

Au under factor 3 with 7.7% variance. Au and Cu were also significantly positively correlated ($r = 0.877$; $p \leq 0.05$) in the talc-chlorite schist, with both elements grouped under factor 3 using the PCA (Tables 4, 5, 6 and 7). Au displayed no positive correlations with other elements in quartzite and amphibolite, mainly due to the fact that its concentration was preponderantly below detection limit in the two lithologies. The groupings of Au and Zn (quartz-biotite schist), and Au and Cu (talc-chlorite schist) tallied with significant positive correlations established from Pearson's correlation matrix. Thus, Zn and Cu can be used as pathfinder elements for Au in quartz-biotite schist and talc-chlorite schist, respectively, in the area.

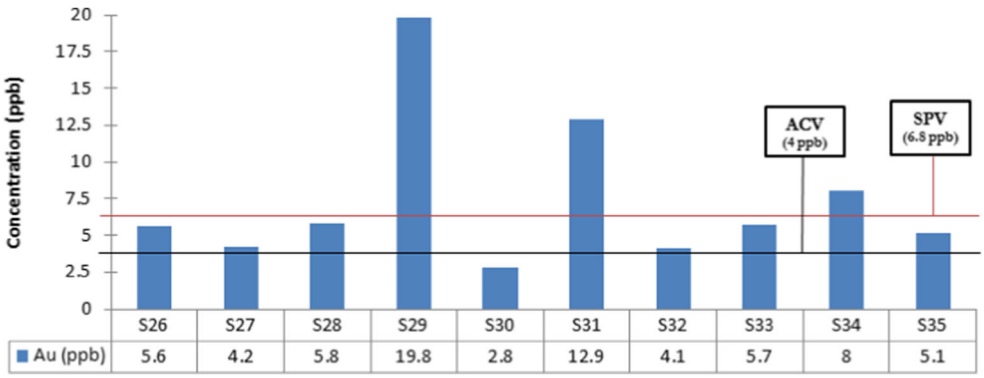



**Fig. 17** Au concentration in Amuta horizontal profile samples compared with ACV and SPV

Pb, Zn, Sb, Hg, Bi and As are often found associated with Au in hydrothermal ore systems (Neacsu et al. 2009; Zhu et al. 2011). Thus, the occurrence of Bi, Ag and Pb (factor 1 for quartz-biotite schist) as well as Hg and Se (factor 1 for talc-

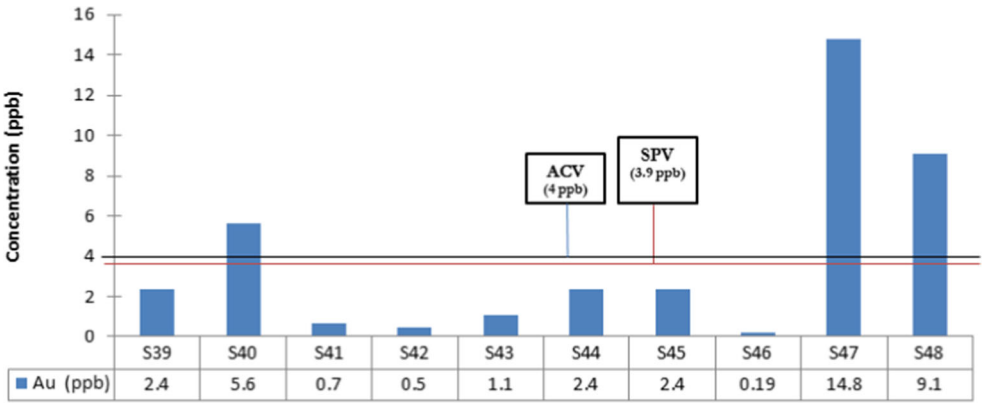



**Fig. 18** The concentration of Au in horizontal profile samples from Itagunmodi relative to ACV and SPV

**Table 4** Inter-elemental correlation in quartz-biotite schist of the area

| | Mo | Cu | Zn | Ni | Cd | Ag | Au | As | Pb | Sb | Se |
|---|---|---|---|---|---|---|---|---|---|---|---|
| Mo | **1** | | | | | | | | | | |
| Cu | 0.911** | 1 | | | | | | | | | |
| Zn | −0.699* | −0.658* | 1 | | | | | | | | |
| Ni | 0.969** | 0.927** | −0.609* | 1 | | | | | | | |
| Cd | −0.557 | −0.229 | 0.220 | −0.569 | 1 | | | | | | |
| Ag | 0.992** | 0.927** | −0.733** | 0.969** | −0.522 | 1 | | | | | |
| Au | −0.320 | −0.277 | **0.704*** | −0.291 | 0.199 | −0.343 | 1 | | | | |
| As | −0.969** | −0.889** | 0.736** | −0.926** | 0.503 | −0.983** | 0.345 | 1 | | | |
| Pb | 0.983** | 0.936** | −0.750** | 0.940** | −0.437 | 0.993** | −0.319 | −0.983** | 1 | | |
| Sb | 0.722** | 0.817** | −0.397 | 0.858** | −0.380 | 0.728** | −0.277 | −0.641* | 0.675* | 1 | |
| Se | −0.557 | −0.229 | 0.220 | −0.569 | 1.000** | −0.522 | 0.199 | 0.503 | −0.437 | −0.380 | 1 |

Correlation is significant at **0.01 level, *0.05 level

**Table 5** Inter-elemental correlation in Osu–Amuta–Itagunmodi talc-chlorite schists

| | Mo | Cu | Zn | Ni | Cd | Au | As | Pb | Sb | Se |
|---|---|---|---|---|---|---|---|---|---|---|
| Mo | 1 | | | | | | | | | |
| Cu | −0.174 | 1 | | | | | | | | |
| Zn | −0.010 | 0.534 | 1 | | | | | | | |
| Ni | 0.196 | 0.475 | 0.970** | 1 | | | | | | |
| Cd | 0.233 | −0.189 | −0.875* | −0.829* | 1 | | | | | |
| Au | −0.364 | **0.877*** | 0.140 | 0.071 | 0.129 | 1 | | | | |
| As | −0.058 | −0.178 | −0.352 | −0.248 | 0.200 | 0.168 | 1 | | | |
| Pb | −0.256 | −0.181 | −0.389 | −0.323 | 0.163 | 0.194 | 0.968** | 1 | | |
| Sb | −0.058 | −0.178 | −0.352 | −0.248 | 0.200 | 0.168 | 1.000** | 0.968** | 1 | |
| Se | 0.233 | −0.189 | −0.875* | −0.829* | 1.000** | 0.129 | 0.200 | 0.163 | 0.200 | 1 |

Correlation is significant at **0.01 level, *0.05 level

**Table 6** Component matrix for trace elements in quartz-biotite schist

| | Component | | |
|---|---|---|---|
| | 1 | 2 | 3 |
| Mo | 0.989 | 0.038 | 0.083 |
| Cu | 0.896 | 0.361 | 0.214 |
| Zn | −0.739 | −0.338 | **0.515** |
| Ni | 0.973 | −0.007 | 0.182 |
| Cd | −0.599 | 0.796 | 0.079 |
| Ag | 0.992 | 0.087 | 0.064 |
| Au | −0.405 | −0.122 | **0.830** |
| As | −0.971 | −0.101 | −0.024 |
| Pb | 0.973 | 0.181 | 0.070 |
| Sb | 0.747 | 0.036 | 0.266 |
| Se | −0.599 | 0.796 | 0.079 |

**Table 7** Component matrix for trace elements in talc-chlorite schist

| | Component | | | |
|---|---|---|---|---|
| | 1 | 2 | 3 | 4 |
| Mo | 0.162 | −0.299 | −0.347 | 0.873 |
| Cu | −0.286 | −0.143 | **0.930** | 0.171 |
| Zn | −0.933 | −0.137 | 0.235 | 0.214 |
| Ni | −0.889 | −0.080 | 0.150 | 0.424 |
| Cd | 0.988 | −0.116 | 0.069 | 0.071 |
| Ag | 0.988 | −0.116 | 0.069 | 0.071 |
| Au | 0.078 | 0.145 | **0.986** | 0.009 |
| As | 0.297 | 0.931 | 0.010 | 0.204 |
| Pb | 0.276 | 0.958 | 0.034 | −0.007 |
| Sb | 0.297 | 0.931 | 0.010 | 0.204 |
| Se | 0.988 | −0.116 | 0.069 | 0.071 |

**Table 8** Correlation matrix for trace elements in Orogo soils

| | Au | Hg | Ag | Cu | Sb | As | Mo | Se | Pb | Zn | Ni | Co | Cd |
|---|---|---|---|---|---|---|---|---|---|---|---|---|---|
| Au | 1 | | | | | | | | | | | | |
| Hg | −0.529 | 1 | | | | | | | | | | | |
| Ag | **0.998*** | −0.577 | 1 | | | | | | | | | | |
| Cu | **0.513** | 0.457 | 0.462 | 1 | | | | | | | | | |
| Sb | −0.794 | 0.936 | −0.828 | 0.115 | 1 | | | | | | | | |
| As | 0.426 | 0.542 | 0.374 | 0.995 | 0.211 | 1 | | | | | | | |
| Mo | 0.039 | 0.827 | −0.019 | 0.878 | 0.577 | 0.92 | 1 | | | | | | |
| Se | **0.747** | 0.169 | 0.707 | 0.954 | −0.189 | 0.92 | 0.693 | 1 | | | | | |
| Pb | −0.783 | 0.942 | −0.817 | 0.133 | 1.000* | 0.229 | 0.591 | −0.171 | 1 | | | | |
| Zn | **0.99** | −0.645 | 0.996 | 0.385 | −0.873 | 0.293 | −0.104 | 0.644 | −0.864 | 1 | | | |
| Ni | **0.912** | −0.134 | 0.887 | 0.82 | −0.475 | 0.76 | 0.445 | 0.954 | −0.459 | 0.844 | 1 | | |
| Co | −0.998* | 0.583 | −1.000** | −0.455 | 0.832 | −0.366 | 0.027 | −0.702 | 0.822 | −0.997* | −0.883 | 1 | |
| Cd | −0.966 | 0.292 | −0.95 | −0.717 | 0.61 | −0.646 | −0.296 | −0.893 | 0.595 | −0.919 | −0.987 | 0.947 | 1 |

Correlation is significant at **0.01 level, *0.05 level

**Table 9** Correlation matrix for trace elements in soils from Amuta area

| | Au | Hg | Ag | Cu | Sb | As | Mo | Se | Pb | Zn | Ni | Co | Cd |
|---|---|---|---|---|---|---|---|---|---|---|---|---|---|
| Au | 1 | | | | | | | | | | | | |
| Hg | 0.386 | 1 | | | | | | | | | | | |
| Ag | −0.755 | 0.314 | 1 | | | | | | | | | | |
| Cu | −0.357 | 0.724 | 0.882 | 1 | | | | | | | | | |
| Sb | −0.195 | 0.83 | 0.79 | 0.986 | 1 | | | | | | | | |
| As | −0.806 | 0.235 | 0.997 | 0.841 | 0.737 | 1 | | | | | | | |
| Mo | 0.339 | −0.737 | −0.873 | −1.000* | −0.989 | −0.83 | 1 | | | | | | |
| Se | **0.714** | −0.371 | −.998* | −0.909 | −0.826 | −0.99 | 0.901 | 1 | | | | | |
| Pb | 0.234 | 0.987 | 0.461 | 0.824 | 0.908 | 0.386 | −0.835 | −0.514 | 1 | | | | |
| Zn | **0.892** | 0.762 | −0.376 | 0.104 | 0.271 | −0.451 | −0.123 | 0.319 | 0.649 | 1 | | | |
| Ni | **0.866** | 0.795 | −0.327 | 0.156 | 0.321 | −0.404 | −0.175 | 0.269 | 0.688 | 0.999* | 1 | | |
| Co | **0.755** | 0.896 | −0.141 | 0.342 | 0.496 | −0.221 | −0.36 | 0.08 | 0.814 | 0.97 | 0.982 | 1 | |
| Cd | −0.491 | 0.614 | 0.942 | 0.989 | 0.95 | 0.911 | −0.986 | −0.961 | 0.732 | −0.044 | 0.009 | 0.2 | 1 |

Correlation is significant at **0.01 level, *0.05 level

**Table 10** Correlation matrix for trace elements in Itagunmodi soils

| | Au | Hg | Ag | Cu | Sb | As | Mo | Se | Pb | Zn | Ni | Co | Cd |
|---|---|---|---|---|---|---|---|---|---|---|---|---|---|
| Au | 1 | | | | | | | | | | | | |
| Hg | −0.384 | 1 | | | | | | | | | | | |
| Ag | 0.2 | 0.828 | 1 | | | | | | | | | | |
| Cu | 0.436 | 0.663 | 0.969 | 1 | | | | | | | | | |
| Sb | **0.911** | −0.731 | −0.223 | 0.026 | 1 | | | | | | | | |
| As | **0.942** | −0.672 | −0.141 | 0.109 | 0.997 | 1 | | | | | | | |
| Mo | **0.767** | −0.887 | −0.476 | −0.243 | 0.963 | 0.938 | 1 | | | | | | |
| Se | **0.989** | −0.24 | 0.346 | 0.567 | 0.838 | 0.88 | 0.661 | 1 | | | | | |
| Pb | **0.782** | 0.276 | 0.767 | 0.902 | 0.454 | 0.527 | 0.199 | 0.867 | 1 | | | | |
| Zn | **0.744** | 0.331 | 0.803 | 0.926 | 0.402 | 0.477 | 0.142 | 0.837 | 0.998* | 1 | | | |
| Ni | **0.999*** | −0.353 | 0.233 | 0.466 | 0.896 | 0.93 | 0.744 | 0.993 | 0.802 | 0.767 | 1 | | |
| Co | −0.191 | 0.98 | 0.924 | 0.8 | −0.579 | −0.509 | −0.777 | −0.04 | 0.463 | 0.513 | −0.158 | 1 | |
| Cd | −0.384 | 1.000** | 0.828 | 0.663 | −0.731 | −0.672 | −0.887 | −0.24 | 0.276 | 0.331 | −0.353 | 0.98 | 1 |

Correlation is significant at **0.01 level, *0.05 level

**Table 11** R-mode factor component matrix for trace elements in Orogo soils

| | Component | | | | |
|---|---|---|---|---|---|
| | 1 | 2 | 3 | 4 | 5 |
| Au | **0.996** | −0.085 | 0 | 0 | 0 |
| Hg | −0.455 | **0.89** | 0 | 0 | 0 |
| Ag | **0.990** | −0.142 | 0 | 0 | 0 |
| Cu | 0.584 | **0.812** | 0 | 0 | 0 |
| Sb | −0.74 | **0.673** | 0 | 0 | 0 |
| As | 0.502 | **0.865** | 0 | 0 | 0 |
| Mo | 0.123 | **0.992** | 0 | 0 | 0 |
| Se | **0.801** | 0.599 | 0 | 0 | 0 |
| Pb | −0.727 | **0.686** | 0 | 0 | 0 |
| Zn | **0.974** | −0.226 | 0 | 0 | 0 |
| Ni | **0.943** | 0.332 | 0 | 0 | 0 |
| Co | −0.989 | 0.15 | 0 | 0 | 0 |
| Cd | −0.984 | −0.176 | 0 | 0 | 0 |

Extraction method: principal component analysis

chlorite schist and factor 2 for quartz-biotite schist) indicated a Au-bearing fluid enriched in these elements introduced into the rocks

In the soil samples obtained from Orogo area, positive correlations were observed for Au/Ag (0.998), Au/Se (0.747), Au/Zn (0.990) and Au/Ni (0.912). These elements were also grouped together under factor 1 of the PCA, accounting for 63.7% of total variance. The relationships established for Au with Zn, Ni and Se by correlation and component matrices further reinforced their pathfinder character for the gold and

**Table 12** R-mode factor component matrix for trace elements in soils from Amuta area

| | Component | |
|---|---|---|
| | 1 | 2 |
| Au | −0.357 | **0.934** |
| Hg | **0.725** | 0.689 |
| Ag | **0.882** | −0.472 |
| Cu | **1** | −0.001 |
| Sb | **0.986** | 0.168 |
| As | **0.84** | −0.543 |
| Mo | −1 | −0.018 |
| Se | −0.909 | 0.417 |
| Pb | **0.825** | 0.565 |
| Zn | 0.105 | **0.994** |
| Ni | 0.157 | **0.988** |
| Co | 0.343 | **0.939** |
| Cd | **0.989** | −0.149 |

Extraction method: principal component analysis

**Table 13** R-mode factor component matrix for trace elements in Itagunmodi soils

| | Component | |
|---|---|---|
| | 1 | 2 |
| Au | **0.96** | 0.281 |
| Hg | −0.628 | **0.778** |
| Ag | −0.084 | **0.996** |
| Cu | 0.166 | **0.986** |
| Sb | **0.99** | −0.14 |
| As | **0.998** | −0.057 |
| Mo | **0.916** | −0.401 |
| Se | **0.906** | 0.423 |
| Pb | 0.575 | **0.818** |
| Zn | 0.527 | **0.85** |
| Ni | **0.95** | 0.313 |
| Co | −0.459 | **0.888** |
| Cd | −0.628 | **0.778** |

Extraction method: principal component analysis

can be used in further studies in exploring for gold within the study area (Amuda et al. 2013). Roberts et al. (1997) have opined that Au formed by hydrothermal process have metal association such as shown in Orogo area. At Amuta, correlation and component matrices established relationships for Au/Se (0.714), Au/Zn (0.892), Au/Ni (0. 866) and Au/Co (0.755), with these elements making up 40% of total variance under factor 2 of PCA. Zn, Ni and Co could hence serve as pathfinder for Au mineralisation in Amuta area. The soils obtained from Itagunmodi area displayed positive correlations for Au/Sb (0.911), Au/As (0.942), Au/Mo (0.767), Au/Se (0.989) and Au/Ni (0.999). Au, Sb, As, Mo, Se and Ni were grouped under factor 1 of the PCA, accounting for 54.6% of total variance (Tables 8, 9, 10, 11, 12, 13). The positive relationships established for Au with Mo, Ni, Pb, Sb and As are suggestive of these elements as Au pathfinders in the area.

Association of Au with metals such as Zn, Ni, Mo, Pb and Co commonly occurs in Au formed by hydrothermal processes (Roberts et al. 1997). Au was observed to correlate with Zn, Ni and Se (Orogo); Zn, Ni and Co (Amuta); and with Ni, Mo, As and Pb (Itagunmodi). The elemental associations observed and the mineralogy of the vertical profile soils corroborates the belief that Au mineralisation in the study area was formed by hydrothermal process.

## Evaluation of additional mineralisation potential

An evaluation of possible additional mineralisation potential was conducted by comparing Au concentrations in rocks and horizontal profile soil samples analysed with those in the average crust, AGM topsoil and saprolitic layers, respectively. This was done to delineate possible anomalous Au zones for

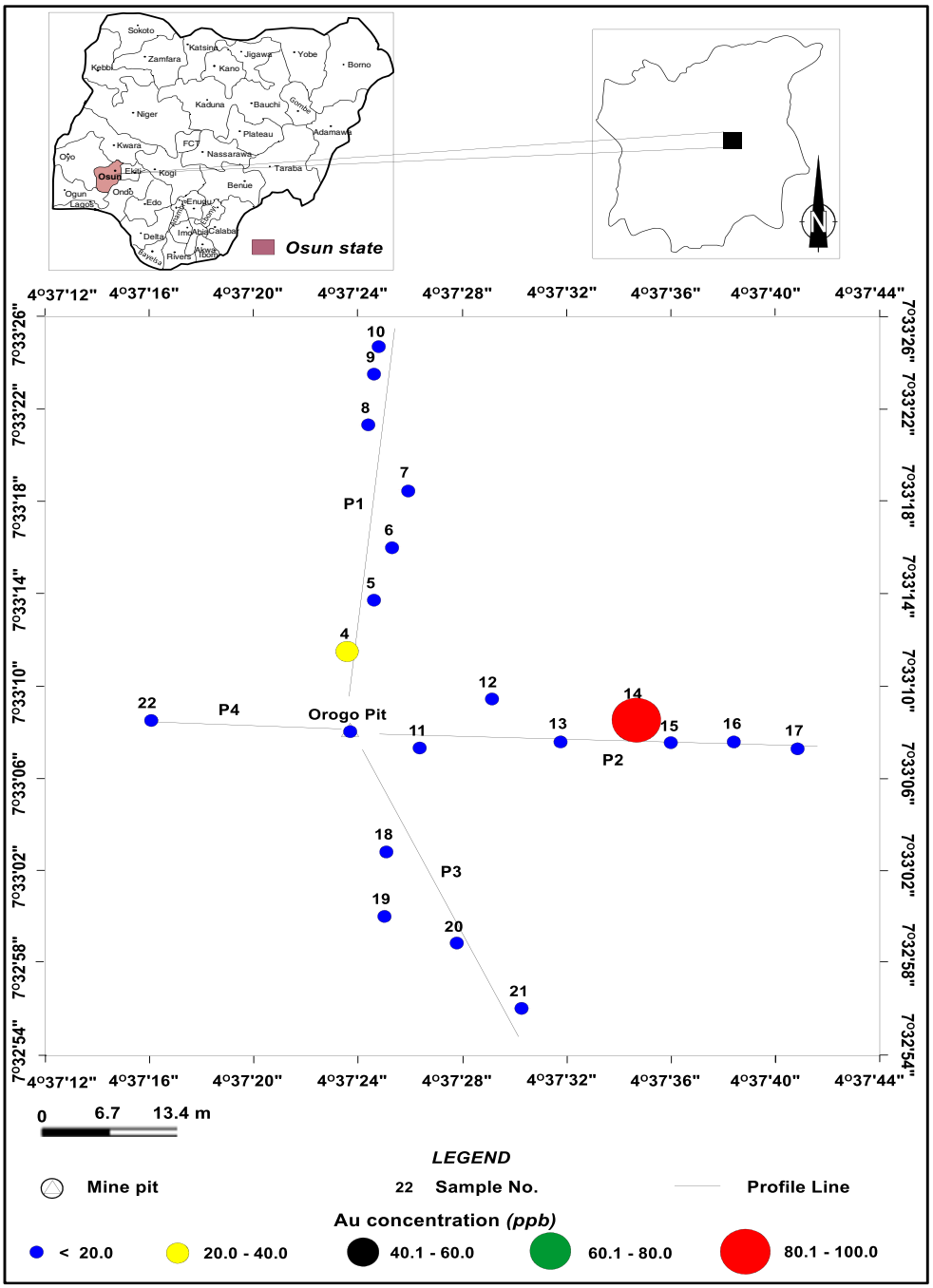



**Fig. 19** Locations of additional Au mineralisation potential within Orogo Area

further investigation and identify additional areas within the eluvium from where Au could be mined.

A comparison of the concentration of Au in rocks with the ACV yielded four (4) anomalous zones (three within quartz-biotite schist lithology, one in the talc-chlorite schist); occurring east of the amphibolite suite, in the eastern half of the study area (Fig. 14). The average composition of Au in the top soils from the three AGM pits (4.6 ppb) falls in the range of the average crustal value of Au. On the horizontal profile from Orogo area, six (6) locations (S04, S13, S14, S15, S17 and S22) had Au concentrations which exceeded the average concentration in top soils of the artisanal mine workings while at Amuta, seven (7) locations (S26, S28, S29, S31, S33, S34 and S35) recorded Au concentrations higher than the average for the artisanal pits. Locations S40, S47 and S48 recorded concentrations higher than the average Au in the Itagunmodi pit. Locations S14 (78.8 ppb) and S20 (20.4 ppb) along the eastern and northern horizontal profiles at Orogo; S29 (19.8 ppb) and S31 (12.9 ppb) along the northeastern and northwestern horizontal profiles at Amuta; and S48 (14.8 ppb) along the north-west

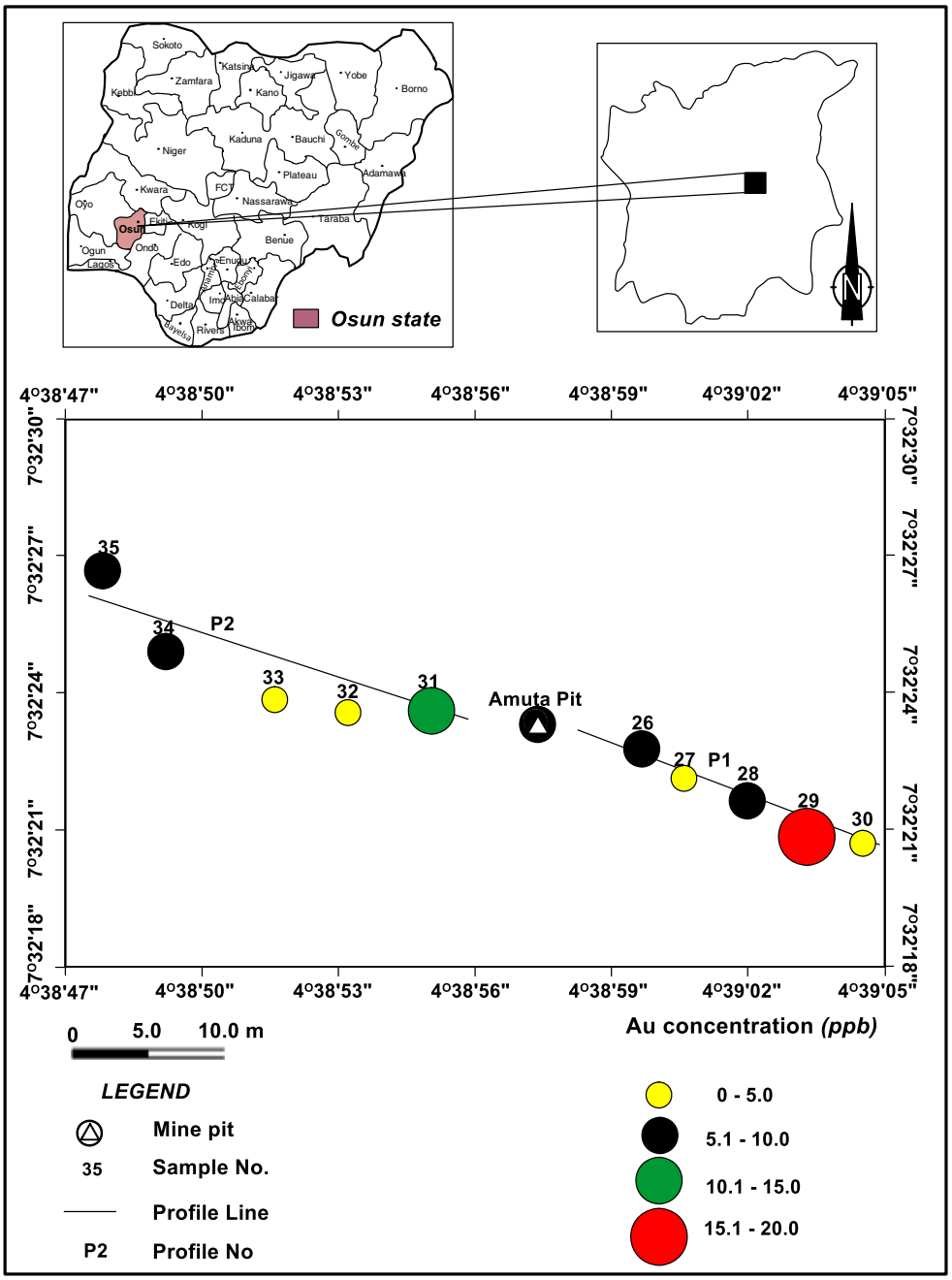



**Fig. 20** Locations of additional Au mineralisation potentials within Amuta Area

horizontal profile at Itagunmodi recorded the highest Au concentrations in samples from the horizontal profiles (Online Resource V, VI and VII; Figs. 19, 20 and 21). Relative to the SPV, however, locations S04, S13, S14 and S15; S29, S31 and S34; and S40, S47 and S48 at Orogo, Amuta and Itagunmodi respectively, displayed anomalous Au concentrations. The evaluation of Au concentration in soils obtained from lateral profiles around the three AGM pits revealed that gold mineralisation extends beyond current artisanal mine workings, with more extensive exploration potentials.

## Conclusion

The study presented hitherto undocumented data on the concentration, distribution and geochemical characteristics of gold mineralisation in rocks and soils of the areas investigated. The Au concentration in the rocks within Osu–Amuta–Itagunmodi areas were in the order quartz-biotite schist > talc-chlorite schist > amphibolite >> quartzite. They displayed low Au abundances relative to the average crust but with four anomalous zones identified in the eastern part of the area.

Gold mining within the area studied is mostly artisanal and principally from eluvial deposits. The artisanal mines are

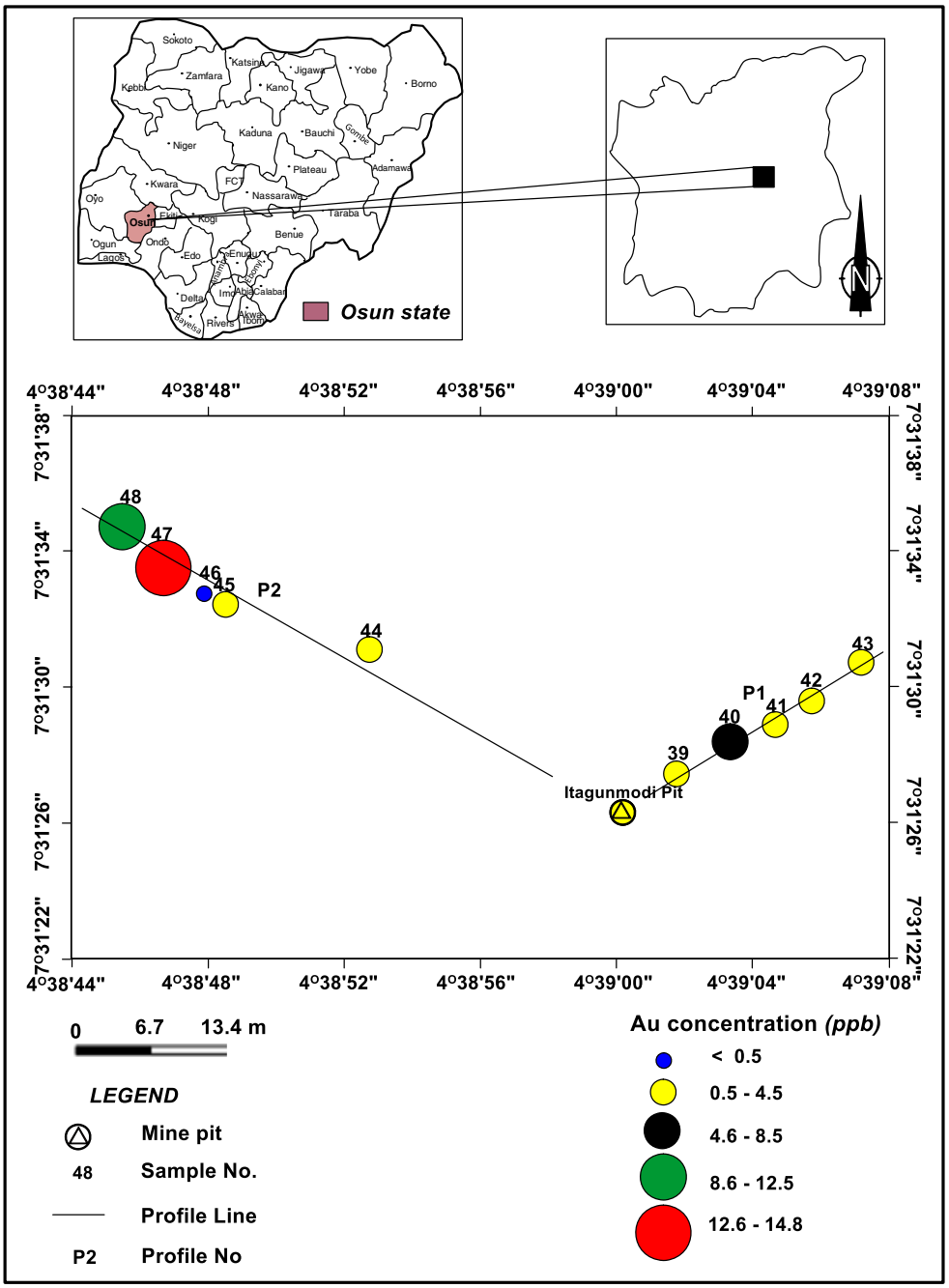



**Fig. 21** Location of additional Au mineralisation potentials within Itagunmodi Area

located predominantly at the bases of slopes and ridges. Field observations revealed that gold is panned from saprolitic layers occurring at depths between 1.5 and 3.5 m in the residual soils overlying quartzite/quartz-biotite schist and amphibolite lithologies. Quartz (34.15–84.91%), with subordinate kaolinite (10.42–38.39%) and hematite (2.40–27.46%), were the dominant minerals in the analysed vertical profile soils, suggestive of hydrothermal alteration of the bedrocks. The association of Au with Zn, Ni, Co, Mo and Pb, evidenced from correlation and component matrices for trace elements in the rocks and soils, further lends credence to the hypothesis that Au mineralisation was through hydrothermal process.

An evaluation of Au concentration in soils obtained from horizontal profile samples around current artisanal mine workings revealed generally higher concentrations when compared with concentrations at the mine pits. This indicated additional mineralisation potential beyond the current artisanal workings and potential for further exploration.

## Recommendations

Core samples should be obtained from the anomalous Au concentration zones identified in the quartz-biotite schist and

talc-chlorite schist east of the amphibolite complex in the study area, for more detailed investigation. Test pits should also be dug to depth at the areas identified along the horizontal profiles as having additional mineralisation potential. This, considering the observed trend of increased Au concentration with depth, should serve to ascertain the additional mineralisation potentials within eluvial deposits in the area.

**Acknowledgements** This study forms part of the first and second authors' research at the Pan African University Life and Earth Sciences Institute (PAULESI), University of Ibadan, sponsored by the African Union Commission. The help rendered by Mr. Bode E. Bankole at the XRD Laboratory of the University of Poitiers in France is invaluable. Dr. Olusegun G. Olisa is gratefully appreciated for his assistance during all phases of the field mapping exercise. The constructive comments of the reviewers are acknowledged with gratitude.

## References

Adepoju MO, Adekoya JA (2011) Reconnaissance geochemical study of a part of Igarra Schist Belt, Southwestern Nigeria. IFE J Sci 13(1): 75–92

Akande SO, Fakorede O, Mucke A (1988) Geology and genesis of gold bearing quartz veins at Bin Yauri and Okolom in the Pan African domain of Western Nigeria. Geol Mijnb 67:41–51

Akinlalu AA, Adelusi AO, Olayanju GM, Adiat KAN, Omosuyi GO, Anifowose AYB, Akeredolu BE (2018) Aeromagnetic mapping of basement structures and mineral characterisation of Ilesa Schist Belt, Southwestern Nigeria. J Afr Earth Sci 138:383–389

Akintola AI, Olorunfemi AO, Bankole SI, Omotoye SJ, Ajayi BO (2013) Petrography and geochemical evaluation of major and trace element concentrations in stream sediments of Itagunmodi and its environs, Southwestern Nigeria. J Earth Sci Geotech Eng 3(4):1–24

Akpan OU, Yakubu TA (2010) A review of earthquake occurrences and observations in Nigeria. Earthq Sci 23:289–294

Amuda AK, Danbatta UA, Najime T (2013) Geology and gold mineralisation around Kutcheri, North-Western Nigeria. IOSR J Appl Geol Geophys 1(6):18–24

Bish DL (1994) Quantitative X-ray diffraction analysis of soils. In: Amonette JE, Zelazny LW (eds) Quantitative methods in soil mineralogy. SSSA Miscellaneous Publication. SSSA, Inc., Madison, pp 267–295

Deer WA, Howie RA, Zussman J (1992) An introduction to the rock-forming minerals. Prentice Hall, London

Garba I (2002) Geochemical characteristics of the gold mineralization near Tsohon Birnin Gwari, Northwestern Nigeria. Chem Erde 62: 160–170

Ministry of Mines and Steel Development (2004) Gold deposits: exploration opportunities in Nigeria

Neacsu A, Popescu GC, Constantinescu B, Vasilescu A, Ceccato D (2009) The geochemical signature of Native Gold from Rosia Montana and Musariu Ore Deposits Metaliferi Mountains (Romania)—preliminary data. Carpathian J Earth Environ Sci 4(1):49–59

Obaje NG (2009) Geology and Mineral Resources of Nigeria. Springer Dordrecht, London

Oke SA, Abimbola AF, Rammlmair D (2014) Mineralogical and geochemical characterisation of gold bearing quartz veins and soils in parts of Maru schist belt area. Northwestern Nigeria, Journal of Geological Research, 17 pp

Oyinloye AO (1995) Geochemistry of the Iperindo Primary Alteration Selvages in Ilesha Area, Southwestern Nigeria. Afr J Sci Technol 7(2):36–42

Oyinloye AO (1997) Ore petrology and chemical compositions of gold and associated sulphides in the Iperindo primary gold deposit in Ilesha Area, Southwestern Nigeria: implications on stages of mineralization. Afr J Sci 1(1):71–81

Oyinloye AO (2002) Au-Ag, K-Rb-Sr and 34S isotope chemical composition of gold deposit in Ilesa Area, Southwestern Nigeria. J Chem Soc Nigeria 27(2):162–166

Oyinloye AO, Steed GM (1996) Geology and geochemistry of Iperindo primary gold deposit, Ilesha schist belt, Southwestern Nigeria. Appl Earth Sci (Trans Instu Min Metall) 105:B74–B81

Roberts F, Poulsen KH, Dube B (1997) Gold deposits and their geological classification. Proceeding of Exploration 97: Fourth Decennial International Conference in Mineral Exploration 209–220

Turekian KK, Wedepohl KH (1961) Distribution of the elements in some major units of the Earth's crust. Bull Geol Soc Am 72:175–192

Wright JB (1985) Geology and Mineral Resources of West Africa. George Allen & Unwin, London

Zhu Y, Umemura T, Haraguchi H, Inagaki K, Chiba K (2009) Determination of REEs in seawater by ICP-MS after on-line preconcentration using a syringe-driven chelating column. Talanta 78:891–895

Zhu Y, An F, Tan J (2011) Geochemistry of hydrothermal gold deposits: a review. Geosci Front 2(3):367–374